Transcellular Route of Diffusion through Stratum Corneum: Results from Finite Element Models

ANA M. BARBERO, H. FREDERICK FRASCH

Health Effects Laboratory, National Institute for Occupational Safety and Health, 1095 Willowdale Road, Morgantown, West Virginia 26505

Received 8 February 2006; revised 9 May 2006; accepted 11 May 2006

Published online in Wiley InterScience (www.interscience.wiley.com). DOI 10.1002/jps.20695

ABSTRACT: Insight into the stratum corneum (SC) permeation pathway for hydrophilic compounds is gained by comparing experimental measurements of permeability and lag time (t_{lag}) with the predictions of a finite element (FE) model. A database of permeability and lag time measurements ($n = 27$) of hydrophilic compounds was compiled from the literature. Transcellular and lateral lipid diffusion pathways were modeled within a brick-and-mortar geometry representing fully hydrated human SC. Modeled t_{lag}'s for the lipid pathway are too brief to account for the experimental quantities, whereas the transcellular pathway with preferential corneocyte partitioning does account for them. Measured t_{lag}'s are highly correlated ($p < 0.0001$) with the compound's octanol-water partition coefficient, supporting the hypothesis of an aqueous-lipid partition mechanism in the permeation of hydrophilic compounds. The importance of the lag time for identifying the diffusion pathway is demonstrated. © 2006 Wiley-Liss, Inc. and the American Pharmacists Association J Pharm Sci 95:2186–2194, 2006

Keywords: skin absorption; diffusion; transdermal; permeability; lag time; mathematical model; partition coefficient

INTRODUCTION

The pathway for diffusion of exogenously applied chemicals through skin will be determined by the physicochemical nature of the diffusing substance and its affinity to the various skin components, and also by the physicochemical nature and structural organization of the skin.[1] Despite decades of research, the preferred path (or paths) for diffusion within the stratum corneum (SC) has not been unequivocally identified.

It is now widely believed that lipophilic compounds will follow the intercellular lipoidal pathway,[2] but the pathway followed by hydrophilic compounds remains more speculative. A highly tortuous polar pathway has been postulated.[3–7] In support, permeation coefficients of these compounds do not correlate with their octanol-water partition coefficients[4] as they do for lipophilics. Furthermore, a possible transfollicular route is generally disregarded because of its small fractional area and because lag times are too long to be accounted for. This polar pathway could be intercellular, possibly through hydrophilic regions present in the lipid layers.[8]

Alternate hypotheses for hydrophilic chemical permeation are the lateral lipid pathway[9,10] and the transcellular pathway that has recently been championed by Kasting.[11,12] This study explores the feasibility of these two potential pathways. Our hypothesis is that experimentally observed lag times of hydrophilic chemicals are too long to be accounted for by the lateral lipid pathway, but that a transcellular route with preferential corneocyte partitioning can account for them. A database of

The findings and conclusions in this report are those of the authors and do not necessarily represent the views of the National Institute for Occupational Safety and Health.

Correspondence to: H. Frederick Frasch (Telephone: 304-285-5755; Fax: 304-285-6041; E-mail: HFrasch@cdc.gov)

Journal of Pharmaceutical Sciences, Vol. 95, 2186–2194 (2006)

measured permeabilities and lag times of hydrophilic compounds is compiled, and results of a finite element (FE) SC diffusion model are compared with these measurements.

METHODS

Finite Element Model

A two-dimensional FE model of diffusion within human SC was created using the software package ANSYS version 7.0 (Ansys, Inc., Canonsburg, PA). Details of the model formulation and solution have been described elsewhere.[13] Briefly, the distribution of concentration in space and time is solved numerically within a 2-D representation of human SC, consisting of two homogeneous phases: corneocytes and lipids. Boundary and initial conditions are applied to the model that mimic *in vitro* diffusion cell experiments. From these results, permeability coefficients and diffusional lag times can be calculated that depend on model geometry, corneocyte-lipid partitioning, and diffusivity within the corneocyte and lipid phases.

Stratum Corneum Geometry

The simplified geometry of a brick-and-mortar representation (Fig. 1) was selected because it has been demonstrated that this geometry adequately represents diffusion within a more complex and realistic heterogeneous SC structure.[13,14] Dimensions of the normal (unswollen) SC are based on typical human SC dimensions that were derived from various sources.[15–18] The normal SC geometry is modified to account for hydration-induced swelling.[19,20] The swollen corneocytes are 44 μm wide (d) and 3.5 μm in thickness (h). They are surrounded by 0.05 μm lipid layer, which makes a lipid layer between corneocytes (s) 0.1 μm thick while the top and bottom lipid layers are 0.05 μm thick. Ten corneocyte layers are included in the model ($n = 10$), which gives a total hydrated SC thickness of 36 μm. The short overlapping section (l_S) is 10.8 μm.

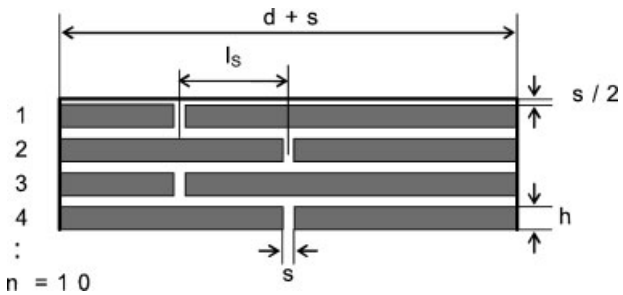

Figure 1. Geometric model of stratum corneum. Diffusion occurs through lipid layers and corneocytes and a partition coefficient is applied between these two phases. d, corneocyte width; h, corneocyte thickness; s, lipid thickness; l_s, length of short overlapping section; n, number of layers.

Corneocyte and Lipid Diffusivites

Corneocytes and lipids are considered to be homogeneous materials with isotropic diffusivities. The diffusion coefficients D_{cor} and D_{lip} are model inputs. Values were chosen to span a wide range of possible experimental values. For the transcellular path, D_{lip} and D_{cor} were varied from 10^{-11} to 10^{-7} cm^2/s; for the lipid pathway, D_{lip} was varied from 10^{-11} to 10^{-5} cm^2/s. For the purposes of the present study, no attempt was made to relate these values to actual diffusivities of specific compounds.

Application of Corneocyte-Lipid Partition Coefficient

At the boundaries between lipid bilayers and corneocytes, it is assumed that spontaneous chemical partitioning occurs. The partition coefficient $K_{cor\text{-}lip}$ is a model input that creates a discontinuity by constraining the following relationship between the concentrations at a boundary between a corneocyte and its surrounding lipid:

$$K_{cor-lip} = \frac{C_{cor}}{C_{lip}} \quad (1)$$

Since the FE method allows only one value for each variable in each spatial location or node, a method must be devised to apply this discontinuity at the boundary. This is achieved using a change of variables in one of the media to account for the partition coefficient. This method is described in detail and validated in Barbero and Frasch.[13]

Boundary and Initial Conditions, and Model Solution

Periodicity is applied at the lateral boundaries to impart infinite dimension in the transverse direction. Other boundary and initial conditions are applied that mimic infinite dose diffusion cell

experiments. The SC is initially free of chemical, and sink conditions are maintained at the lower surface. At the upper surface, a constant concentration is imposed at time 0 and maintained for the duration of the simulation. The results obtained are concentration distributions throughout the SC as a function of time, the spatially averaged flux at the lower surface of the SC as a function of time, and the time integral of the flux (mass accumulation per unit area). Permeability (k_p) is calculated as the steady-state flux divided by the imposed concentration. Lag times (t_{lag}) are calculated by extrapolation of the steady-state portion of the mass accumulation curve to the time axis:

$$t_{lag} = \frac{J_{ss}T - Q_T}{J_{ss}} \quad (2)$$

where J_{ss} is steady-state flux, Q_T is total mass accumulation over the entire simulation time T, which in all cases was at least 10 times the lag time. This method is consistent with the general definition of lag time given by Frisch.[21]

Finite element diffusion simulations were run with $K_{cor\text{-}lip}$ values in the range from 0 to 10^4, and for different combinations of corneocyte and lipid diffusivities. With $K_{cor\text{-}lip} = 0$, permeant is confined within the lipid layers.[14] For each value of $K_{cor\text{-}lip}$, six to nine runs were performed with different combinations of diffusivities in both lipid and corneocytes to produce the results shown in Figure 2.

Database of Permeabilities and Lag Times of Hydrophilic Compounds

Knowledge of both permeability and lag time for permeants provides insight into the potential permeation pathway.[22] Unfortunately there are not many experimental lag times reported in the literature. Twenty-seven reported values for hydrophilic compounds (log $K_{ow} \lesssim 0$) are given in Table 1. The listed compounds include amino acids,[4] glycol-ethers,[23] mannitol,[24,25] sucrose,[25] water,[26] urea,[22] caffeine,[27] methanol,[27] nicotinamide,[11] several model drugs used to study the effect of penetration enhancers,[28–30] and nonsteroidal anti-inflammatory drugs.[31] These data were generated from both human and animal skin and most were obtained using an aqueous vehicle.

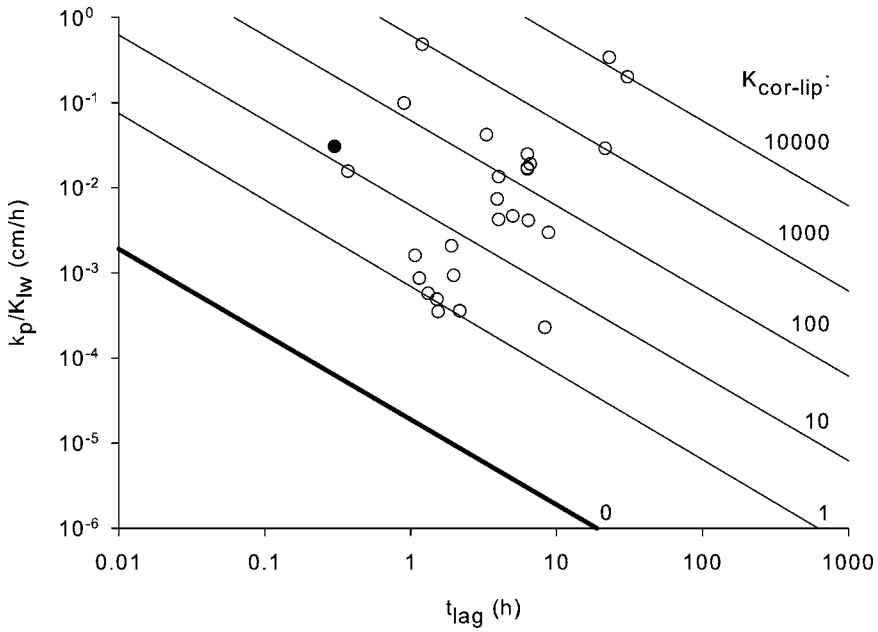

Figure 2. Transcellular diffusion through swollen SC model. FE results for corneocyte-lipid partition coefficient ($K_{cor\text{-}lip}$) values from 0 to10^4 and different combinations of diffusivities are plotted as continuous lines. $K_{cor\text{-}lip} = 0$ (thicker line) corresponds to the exclusively lipid pathway. Experimental values from Table 1 are plotted with circles. Water is shown as a closed circle.

 DOI 10.1002/jps

Table 1. Permeabilities and Lag Times of Hydrophilic Compounds

Compound	MW	Log K_{ow}	Log $K_{cor\text{-}lip}$	k_p (cm/h)	t_{lag} (h)	K_{lw}	k_p/K_{lw} (cm/h)	Ref.
DPGME[a]	148.2	−0.35	0.00	1.1e-4	1.51	2.24e-1	4.9e-4	23
DPGME 50%[a]	148.2	−0.35	0.15	8e-5	2.17	2.24e-1	3.6e-4	23
EGNPE[a]	104.2	0.08	0.18	4.3e-4	1.15	4.99e-1	8.6e-4	23
EGNPE 50%[a]	104.2	0.08	0.85	1.03e-3	1.90	4.99e-1	2.06e-3	23
EGIPE[a]	104.2	0.05	0.08	2.7e-4	1.32	4.72e-1	5.7e-4	23
EGIPE 50%[a]	104.2	0.05	0.48	4.4e-4	1.97	4.72e-1	9.3e-4	23
EGMEA[a]	118.1	0.10	0.48	8.3e-4	1.07	5.18e-1	1.6e-3	23
EGMEA 50%[a]	118.1	0.10	−0.05	1.81e-4	1.54	5.18e-1	3.49e-4	23
Aspartic acid[b]	133.1	−3.47	4.00	1.33e-4	30.6	6.65e-4	2.00e-1	4
Lysine[b]	146.2	−3.05	4.15	4.9e-4	23.0	1.46e-3	3.4e-1	4
Histidine[b]	155.2	−2.90	3.00	5.54e-5	21.5	1.93e-3	2.88e-2	4
Water[c]	18.0	−1.38[38]	1.20	1e-3	0.3	3.28e-2	3.1e-2	26
Nicotinamide[d]	122.0	−0.37	0.48	4.9e-5	8.3	2.16e-1	2.3e-4	11
Mannitol[e]	182.2	−3.10[38]	2.00	1.78e-5	4	1.33e-3	1.34e-2	24
Mannitol[f]	182.2	−3.10	2.30	5.54e-5	3.3	1.33e-3	4.18e-2	25
Sucrose[f]	342.3	−2.34	1.70	4.01e-5	3.9	5.47e-3	7.33e-3	25
Tegafur (60/40 Et/w)[g]	200.2	−0.48	2.26	3.0e-3	6.3	1.76e-1	1.7e-2	28
Tegafur (60/40 Et/w)[h]	200.2	−0.48	2.23	2.9e-3	6.3	1.76e-1	1.7e-2	29
Tegafur[h]	200.2	−0.48	1.70	5.2e-4	8.8	1.76e-1	3.0e-3	29
5-Fluorouracil (60/40Et/w)[g]	130.1	−0.95[38]	2.48	1.8e-3	6.3	7.31e-2	2.5e-2	30
Caffeine(60/40 Et/w)[g]	194.2	−0.07[38]	1.60	1.75e-3	5.0	3.77e-1	4.64e-3	30
Theophyline (60/40 Et/w)[g]	180.2	−0.02[38]	1.70	1.7e-3	6.4	4.14e-1	4.1e-3	30
Tenoxicam[i]	337.4	−0.40	2.18	2.0e-2	0.9	2.04e-1	9.8e-2	31
Ketorolac[i]	255.3	−0.05	3.00	1.90e-1	1.2	3.92e-1	4.85e-1	31
Urea[j]	60.1	−2.11[38]	2.30	1.6e-4	6.6	8.40e-3	1.9e-2	22
Methanol[j]	32.0	−0.77[38]	1.00	1.6e-3	0.37	1.02e-1	1.6e-2	27
Caffeine[j]	194.2	−0.07[38]	1.78	1.6e-3	4.0	3.77e-1	4.2e-3	27

MW, molecular weight; log K_{ow}, base 10 logarithm of the octanol-water partition coefficient. Unless otherwise noted, the value comes from the cited reference; log $K_{cor\text{-}lip}$, base 10 logarithm of the modeled corneocyte-lipid partition coefficient; k_p, permeability coefficient; t_{lag}, lag time; K_{lw}, lipid-water partition coefficient (Eq. 3); ref., reference.

[a]DPGME, dipropylene glycol (mono) methyl ether; EGNPE, ethylene glycol (mono) n-propyl ether; EGIPE, ethylene glycol (mono) iso-proppyl ether; EGMEA, ethylene glycol (mono) methyl ether acetate. Full thickness human skin. Both neat and 50% aqueous solutions.

[b]Dermatomed human skin. Aqueous vehicle. Only data of zwitterionic amino acids, (no net charge), are included.

[c]Heat separated human epidermal membranes. Aqueous vehicle.

[d]Heat separated human epidermal membranes. Aqueous vehicle. Several values of membrane characteristic time are reported depending on experimental conditions. Lag time given here based on permeation studies.

[e]Full thickness pig skin. Aqueous vehicle. Lag time estimated from graph.

[f]Full thickness pig skin. Aqueous vehicle. Permeabilites taken as average of those measured from 20 to 48 h.

[g]Full thickness hairless mouse skin. 60/40, ethanol/water vehicle. k_p calculated from cumulative percentage penetration rate.

[h]Full thickness hairless mouse skin. Both aqueous and 60/40 ethanol/water vehicle solutions. Permeability calculated from reported flux measurements.

[i]Dermatomed human skin. Aqueous vehicle.

[j]Heat separated human stratum corneum. Aqueous vehicle.

Application of Lipid-Water Partition Coefficient

A lipid-water partition coefficient, K_{lw}, is used to account for the ratio of the equilibrium concentrations in the SC lipids, C_{lip}, to the concentration in the surrounding aqueous vehicle, C_w. The following power law relationship for K_{lw} has been proposed by various authors:

$$K_{lw} = \frac{C_{lip}}{C_w} = cK_{ow}^{\beta} \quad (3)$$

where K_{ow} is the octanol-water partition coefficient and c and β are (usually) empirical constants. Nitsche et al.[32] recently proposed $c = 0.43$ and $\beta = 0.81$, based upon regression of 72 data

points, most of which, however, were lipophilic. To compare permeabilities of specific compounds to FE model results, the experimental permeabilities are divided by the compound's lipid-water partition coefficient calculated from Eq. 3.

RESULTS

Table 1 lists information relevant to the hydrophilic compounds compiled here. In addition to experimentally reported k_p and t_{lag}, the table presents molecular weights, octanol-water partition coefficients, calculated K_{lw} (Eq. 3) and modeled $K_{cor\text{-}lip}$. The latter have been estimated by interpolation of the experimental values between modeled results.

The relationship between permeability and lag time was investigated. For a homogeneous membrane, an inverse relationship exists between the two. Since k_p is proportional to the ratio D/h and t_{lag} is proportional to h^2/D, where h is membrane thickness, a linear relationship with negative slope on a log-log plot results as diffusivity D is varied. For a fixed corneocyte-lipid partition coefficient, the FE results also generate a straight line ($r^2 > 0.998$) on a log-log plot of lag time versus permeability, over a broad range and combination of diffusivities in the lipid and corneocyte phases that was examined. The lines are nearly parallel (slopes within 2% of each other) for different $K_{cor\text{-}lip}$'s. A linear fit was applied to the results to group the values corresponding to each partition coefficient (Fig. 2). The implication of a linear fit is that, for a given $K_{cor\text{-}lip}$, the effective diffusional path length of the modeled membrane is nearly constant. This result confirms findings from previous model studies.[14,33]

In order to explore the relationship between experimental values of k_p and t_{lag} and model predictions of *possible* corneocyte-lipid partition coefficients for these specific compounds, the experimental values of hydrophilic compounds from Table 1 are plotted along with FE results using the swollen SC geometry (Fig. 2). This comparison tests the hypothesis that the experimental lag times are too long to be accounted for by the lateral lipid pathway but can be accounted for by the transcellular pathway.

We also examined nonswollen SC geometry. Results (not shown) did not differ much from those displayed in Figure 2. The lines of constant $K_{cor\text{-}lip}$ were shifted down slightly, so that a given compound was modeled using ~twofold higher value of $K_{cor\text{-}lip}$.

A specified point on the k_p versus t_{lag} plot is not defined by a unique combination of D_{cor} and D_{lip}. This is illustrated using a specific compound, water. Measured values of k_p and t_{lag} for water are satisfied by a corneocyte-lipid partition coefficient of about 16 (Fig. 2). Figure 3 shows the FE modeled range of D_{lip} and D_{cor} that produces the measured k_p and t_{lag} values (with small (<3%) variance), while keeping $K_{cor\text{-}lip} = 16$. The symbol on Figure 3 corresponds to the values estimated by Kasting et al. [12] using a simpler multilayer model.

Favorable partitioning of a chemical within the corneocyte phase compared to the lipid phase generally results in an increased lag time for chemical permeation.[34] If this model is correct, and further if one posits an inverse relationship between $K_{cor\text{-}lip}$ and K_{ow}, then a significant negative correlation should exist between t_{lag} and log K_{ow}. The Pearson Product Moment Correlation was used to test the strength of association between the variables t_{lag} and log K_{ow} given in Table 1. (SigmaStat 3.1, Systat Software Inc., Point Richmond, CA). The correlation r between t_{lag} and log K_{ow} is -0.65, which is highly significant ($p < 0.0001$, $n = 27$). No such correlation exists between t_{lag} and molecular weight ($r = 0.08; p > 0.6$).

Although the observed correlation of t_{lag} with log K_{ow} is highly significant, it is strongly influenced by the few measurements of very long lag times reported for amino acids in one study (Tab. 1). If these are removed, the significance disappears.

DISCUSSION

The specific permeation pathway(s) of the SC have not been unequivocally established. Model results described here challenge the hypothesis that hydrophilic compounds permeate via the lateral lipid pathway. Figure 2 demonstrates that the observed lag times are too long to be accounted for by this path (corresponding to $K_{cor\text{-}lip} = 0$). Given the specific combinations of lag times and permeabilities for the hydrophilic compounds that have been measured by others and presented in Table 1, Figure 2 shows that a transcellular permeation pathway can account for these experimental data. Furthermore, Figure 2 demonstrates that for a particular experimental combination of t_{lag} and k_p, the model dictates a unique value of $K_{cor\text{-}lip}$ that is required for

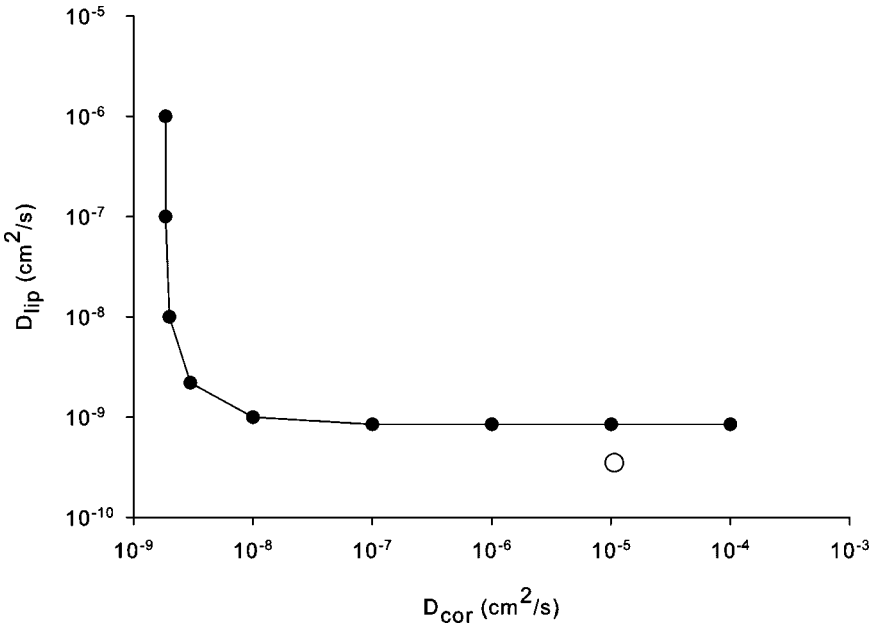

Figure 3. Water diffusivity in the corneocyte versus in the lipid. These combined values and a corneocyte-lipid partition coefficient of 16 give a lag time of 20 min and a permeability 1×10^{-3} cm/h (with variances <3%). Kasting et al.'s[12] model-based calculated values for water are shown with an open circle.

transcellular permeation of the specific compound. These values have been tabulated in Table 1. For all but one of the hydrophilic compounds studied, preferential corneocyte partitioning ($\log K_{\text{cor-lip}} > 0$) is required to obtain the experimental results.

The FE model incorporates a lipid layer on both top and bottom, and the modeled permeability results are obtained for a concentration or boundary condition applied to the top layer of this lipid phase. On the other hand, experimental permeability data are based on the concentration in the vehicle at the surface of the skin membranes. To compare model with experimental results, therefore, requires incorporation of a lipid-water partition coefficient to account for the ratio of the equilibrium concentrations in the SC lipids to the concentration in the aqueous vehicle. Several authors have proposed the relationship given by Eq. 3. We have selected the parameters presented by Nitsche et al.[32] as being representative of the most recent and thorough analysis. Several other published parameters were tested (data not shown), and while the details changed, the fundamental result of Figure 2 remained the same: the combined reported lag times and permeabilities for hydrophilic compounds cannot be accounted for by the lateral lipid pathway, but they can be by a transcellular pathway with a specific modeled corneocyte-lipid partition coefficient.

Lag times are generally measured by extrapolating the steady-state portion of the mass accumulation curve to the time axis. Problems with their measurement are well known and particularly troublesome for long lag times such as those tabulated here. Insufficient experimental time to establish a steady-state rate of permeation, a time-varying increase in membrane permeability due to hydration, depletion of donor permeant, and apparatus lag times using flow-through cells, are some potential difficulties. Except for the last problem, these would lead to an underestimation of the true lag time. All diffusion cells used in the cited studies were of the static type, which the study authors claimed were well stirred.

Further uncertainty is added by the fact that both human and animal data are included in Table 1. Six measurements were made using mouse skin, while the other nonhuman skin was from the pig which is widely regarded as being an excellent model for human skin. The correlation between t_{lag} and $\log K_{\text{ow}}$ improved slightly ($r = -0.69$ vs. $r = -0.65$) with the mouse measurements removed. On the other hand, the correlation between t_{lag} and $\log K_{\text{ow}}$ did not improve when the time lags were normalized by the square of the thickness of SC for the different species. (The

rationale is that t_{lag} is proportional to the square of thickness for a homogeneous membrane.) The SC thickness of mouse and pig were reported by Montiero-Riviere et al.[35] and human SC thickness was taken from Holbrook and Odland.[36] This finding may not be surprising, since it has been noted that the rate of percutaneous penetration does not correlate with skin thickness or number of cell layers.[15] Corneocyte alignment may play a more crucial role in the determination of relative lag times among species.[14] Overall, the observation that lag times of hydrophilic compounds are too long to be explained by the lateral lipid pathway mechanism appears valid even if the lag time measurements may be problematic.

The model presented here explores only two of the potential permeation pathways for hydrophilic compounds. The present model does not include the skin appendage pathway (hair follicles and sweat ducts) that could be important at early exposure times,[19,26] although it may not be significant overall due to its small fractional area. Addition of such a high diffusivity shunt pathway would presumably increase the permeability, but reduce the lag time or create a two-phase lag time that has been observed by some.[11]

Several authors have proposed the existence of a porous polar pathway for hydrophilic compounds.[3–8] Current thinking suggests that this may consist of structural imperfections within the lipid lamellae, but the path does not involve a lipid transport process. Such a pathway is believed to be highly tortuous and would increase lag time[22] (relative to the lateral lipid pathway), and thus may not be distinguishable from the presently modeled transcellular route. Two observations relating to the current data are relevant, however. First, the data tentatively support an aqueous-lipid partitioning mechanism in the permeation of hydrophilic compounds. Second, a proposed dependence of decreasing pore tortuosity with increasing molecular radius[7] would presumably lead to an inverse correlation between lag time and molecular weight for the porous polar pathway. Such a correlation was not found in the data ($r = 0.08; p > 0.6$). However, it should be noted that the molecular weight range of the compounds in Table 1 is quite narrow compared with that studied by Tezel and Mitragotri,[7] and therefore the present data may not exhibit a broad enough range to reveal such a correlation.

The observation that experimental lag times are correlated with octanol-water partition coefficients would suggest that some sort of aqueous-lipid partitioning occurs in the permeation of hydrophilic compounds. One possibility is the transcellular pathway, an older hypothesized mechanism[26] which has recently been revived by Kasting,[11,12] and which is supported by the modeling results presented here. The process of successive partitioning between corneocytes and lipid layers, along with appropriate molecular mobilities within the two phases, results in lag times that agree with measured values.

It is necessary to point out that the observed correlation of t_{lag} with $\log K_{\mathrm{ow}}$ is strongly influenced by the few measurements of very long lag times reported for amino acids (Tab. 1). It would therefore be beneficial to obtain additional measurements of permeabilities and lag times for hydrophilic compounds, in order to confirm or refute this correlation.

The current model is limited in that it considers lipid transport to be isotropic. Recent models highlight the importance of a transbilayer transport mechanism, which is slower than lateral lipid transport, in both lipid[6] and transcellular[37] pathways. The effect of this process on the relationship between modeled permeability and lag time is unknown, and could be an important area for future study.

CONCLUSION

Finite element results presented here support the proposed transcellular pathway for permeation of hydrophilic chemicals. A SC diffusion model, which allows for a transcellular diffusion pathway with preferred corneocyte partitioning, is capable of predicting the long lag times associated with polar permeants including water.

REFERENCES

1. Flynn GL. 1989. Mechanism of percutaneous absorption from physicochemical evidence. In: Bronaugh RL, Maibach HI, editors. Percutaneous absorption: Mechanisms, methodology, drug delivery, 2nd edition. New York: Marcel Dekker. pp 702–747.
2. Hadgraft J. 2004. Skin deep. Eur J Pharm Biopharm 58:291–299.
3. Peck KD, Ghanem A-H, Higuchi WI. 1994. Hindered diffusion of polar molecules through and effective pore radii estimates of intact and ethanol treated human epidermal membrane. Pharm Res 11:1306–1314.

4. Sznitowska M, Berner B. 1995. Polar pathway for percutaneous absorption. In: Surber C, Elsner P, Bircher AJ, editors. Exogenous dermatology, Vol. 22. Curr Prob Dermatol. Basel: Karger. pp 164–170.
5. Sznitowska M, Janicki S, Williams AC. 1998. Intracellular or intercellular localization of the polar pathway of penetration across stratum corneum. J Pharm Sci 87:1109–1114.
6. Mitragotri S. 2003. Modeling skin permeability to hydrophilic and hydrophobic solutes based on four permeation pathways. J Control Release 86:69–92.
7. Tezel A, Mitragotri S. 2003. On the origin of size-dependent tortuosity for permeation of hydrophilic solutes across the stratum corneum. J Control Release 86:183–186.
8. Menon GK, Elias PM. 1997. Morphologic basis for a pore-pathway in mammalian stratrum corneum. Skin Pharmacol 10:235–246.
9. Potts RO, Francoeur ML. 1991. The influence of stratum corneum morphology on water permeability. J Invest Dermatol 96:495–499.
10. Johnson ME, Blankschtein D, Langer R. 1997. Evaluation of solute permeation through the stratum corneum: Lateral bilayer diffusion as the primary transport mechanism. J Pharm Sci 86:1162–1172.
11. Kasting GB, Miller MA, Talreja PS. 2005. Evaluation of stratum corneum heterogeneity. In: Bronaugh RL, Maibach HI, editors. Percutaneous absorption: Drugs, cosmetics, mechanisms, methodology, 4th edition. Boca Raton: Taylor & Francis. pp 193–212.
12. Kasting GB, Barai ND, Wang T-F, Nitsche JM. 2003. Mobility of water in human stratum corneum. J Pharm Sci 92:2326–2340.
13. Barbero AM, Frasch HF. 2005. Modeling of diffusion with partitioning in stratum corneum using a finite element model. Ann Biomed Eng 33:1281–1292.
14. Frasch HF, Barbero AM. 2003. Steady-State flux and lag time in the stratum corneum lipid pathway: Results from finite element models. J Pharm Sci 92: 2196–2207.
15. Elias PM, Cooper ER, Korc A, Brown BE. 1981. Percutaneous transport in relation to stratum corneum structure and lipid composition. J Invest Dermatol 76:297–301.
16. Menton DN. 1976. A minimum-surface mechanism to account for the organization of cells into columns in the mammalian epidermis. Am J Anat 145:1–21.
17. Mershon MM. 1975. Barrier surfaces of skin. In: Baier RE, editor. Applied chemistry at protein interfaces. Washington: American Chemical Society. pp 41–73.
18. Wildnauer R, Miller DL, Humphries WT. 1975. A physicochemical approach to the characterization of stratum corneum. In: Baier RE, editor. Applied chemistry at protein interfaces. Washington: American Chemical Society. pp 74–124.
19. Scheuplein RJ. 1978. Skin permeation. In: Jarrett A, editor. The physiology and pathophysiology of the skin, Vol. 5. New York: Academic Press. pp 1669–1752.
20. Talreja PS, Kasting GB, Kleene NK, Pickens WL, Wang T-F. 2001. Visualization of the lipid barrier and measurements of lipid path length in human stratum corneum. AAPS Pharm Sci 3. Article 13 (http://www.pharmsci.org).
21. Frisch HL. 1957. The time lag in diffusion. J Phys Chem 61:93–95.
22. Li SK, Suh W, Parikh HH, Ghanem AH, Mehta SC, Peck KD, Higuchi WI. 1998. Lag time data for characterizing the pore pathway of intact and chemically pretreated human epidermal membrane. Int J Pharm 170:93–108.
23. Venier M, Adami G, Larese F, Maina G, Renzi N. 2004. Percutaneous absorption of 5 glycol ethers through human skin in vitro. Toxicol In Vitro 18:655–671.
24. Tezel A, Sens A, Mitragotri S. 2003. Description of transdermal transport of hydrophilic solutes during low-frequency sonophoresis based on a modified porous pathway model. J Pharm Sci 92:1–13.
25. Tang H, Blankschtein D, Langer R. 2002. Prediction of steady-state skin permeabilities of polar and nonpolar permeants across excised pig skin based on measurements of transient diffusion: Characterization of hydration effects on skin porous pathway. J Pharm Sci 91:1891–1907.
26. Scheuplein RJ. 1965. Mechanism of percutaneous absorption I. Routes of penetration and the influence of solubility. J Invest Dermatol 45:334–346.
27. Southwell D, Barry BW, Woodford R. 1984. Variations in permeability of human skin within and between specimens. Int J Pharm 18:299–309.
28. Lee CK, Uchida T, Kitagawa K, Yagi A, Akira Y, Kim N-S, Goto S. 1993. Effect of hydrophilic and lipophilic vehicles on skin permeation of tegafur, alclofenac and ibuprofen with or without permeation enhancers. Biol Pharm Bull 16:1264–1269.
29. Lee CK, Uchida T, Noguchi E, Kim N-S, Goto S. 1993. Skin permeation enhancement of tegafur by ethanol/panasate 800 or ethanol/water binary vehicle and combined effect of fatty acids and fatty alcohols. J Pharm Sci 82:1155–1159.
30. Lee CK, Uchida T, Kitagawa K, Yagi A, Kim N-S, Goto S. 1994. Relationship between lipophilicity and skin permeability of various drugs from an ethanol/water/lauric acid system. Biol Pharm Bull 17:1421–1424.
31. Cordero JA, Alarcon L, Escribano E, Obach R, Domenech J. 1997. A comparative study of the transdermal penetration of a series of nonsteroidal antiinflamatory drugs. J Pharm Sci 86:503–508.

32. Nitsche JM, Want T-F, Kasting GB. 2006. A two-phase analysis of solute partitioning into the stratum corneum. J Pharm Sci 95:649–666.
33. Frasch HF. 2002. A random walk model of skin permeation. Risk Anal 22:265–276.
34. Heisig M, Lieckfeldt R, Wittum G, Mazurkevich G, Lee G. 1996. Non steady-state descriptions of drug permeation through stratum corneum. I. The biphasic brick-and-mortar model. Pharm Res 13:421–426.
35. Montiero-Riviere NA, Bristol DG, Manning TO, Rogers RA, Riviere JE. 1990. Interspecies and interregional analysis of the comparative histologic thickness and laser Doppler blood flow measurements at five cutaneous sites in nine species. J Invest Dermatol 95:582–586.
36. Holbrook KA, Odland GF. 1974. Regional differences in the thickness (cell layers) of the human stratum corneum: An ultrastructural analysis. J Invest Dermatol 62:415–422.
37. Wang T-F, Kasting GB, Nitsche JM. 2006. A multiphase microscopic diffusion model for stratum corneum permeability. I. Formulation, solution, and illustrative results for representative compounds. J Pharm Sci 95:620–648.
38. Hansch C, Leo A, Hoekman D. 1995. Exploring QSAR: hydrophobic, electronic, and steric constants. Washington DC: American Chemical Society.